

Lennaert Wouters<sup>1</sup>, Albert Minj<sup>1,2</sup>, Umberto Celano<sup>1</sup>, Thomas Hantschel<sup>1</sup>,  
Wilfried Vandervorst<sup>1,2</sup>, Kristof Paredis<sup>1</sup>

<sup>1</sup>IMEC, Leuven, Belgium

<sup>2</sup>Department of Physics and Astronomy, University of Leuven, Leuven, Belgium

# Carrier Profiling in High Vacuum Using Scanning Spreading Resistance Microscopy and Scanning Capacitance Microscopy

## Introduction

**Scanning Spreading Resistance Microscopy (SSRM)** and **Scanning Capacitance Microscopy (SCM)** are both established scanning probe-based methods for two-dimensional carrier profiling. Their initial development was mainly pushed by the microelectronics industry looking for 2D alternatives for their 1D carrier/dopant profiling techniques, such as Capacitance-Voltage (C-V) measurements, Secondary Ion Mass Spectrometry (SIMS), and Scanning Resistance Profiling (SRP).

In **SSRM**, the resistance of the current spreading through the nanoscale tip-sample contact is measured while scanning the probe. The key to its large sensitivity and spatial resolution lies in the presence of a pressure induced metallic pocket below the tip apex resulting in a (nearly) ohmic tip sample contact. As a result, the measured resistance is dominated by the spreading resistance and hence dependent on the local sample resistivity  $\rho$ :

$$R_{\text{spreading}} = \rho / 4a,$$

Where  $a$  represents the contact size. The main advantages of SSRM include a very high spatial resolution ( $\sim 1$  nm) and a large sensitivity and dynamic range ( $10^{14}$ - $10^{20}$  cm<sup>-3</sup>).

In **SCM**, small capacitance variations ( $\sim 10^{-21}$  F) between the tip and the sample are measured using a high frequency capacitance sensor while scanning the probe. Highly doped regions show a low differential capacitance  $dC/dV$ , while lowly doped areas exhibit a relatively larger capacitance change. The main advantages are the large dynamic range and the carrier type sensitivity as n- and p-type show opposite phases in their  $dC/dV$  signals.

In both methods, it is not straightforward to convert the measured values directly into quantitative values for carriers because detailed information on the probe and sample surface are missing. Hence, a calibration against a known standard is generally the most straightforward way for converting resistance/differential capacitance to resistivity/carrier concentrations.

In fact, both techniques exhibit pros and cons, but are quite complementary; SSRM provides the highest spatial resolution while SCM provides carrier type sensitivity.

As current state-of-the-art devices are entering the sub 10 nm nodes, the requirements for materials and device characterization are being pushed to their limits, requiring every aspect of the measurement to be optimized for successful measurements, for instance the probe, the sample preparation, and the measurement environment.

In this application note, we review the performance of the Park NX-Hivac atomic force microscope (AFM) from Park Systems [1] for SSRM and SCM applications, based on the following three samples:

1. A p-type doped silicon calibration sample (imec CS08-SiB): a sample consisting of various Boron doped epitaxial silicon layers ( $\sim 600$  nm) with known doping concentration (Figure 1).
2. An n-type doped silicon calibration sample (imec CS01-SiAs): a sample consisting of various arsenic doped epitaxial silicon layers with known doping concentration (Figure 5). This sample additionally has a p-type doped layer embedded in the stack.

- Buried oxide sample: a 0.5 nm oxide layer sandwiched in between a highly doped Si and a poly Si layer (Figure 2).

These samples are measured on the Park NX-Hivac AFM system, operating in vacuum conditions ( $\sim 5 \times 10^{-5}$  mbar) using imec Full Diamond probes [2].

## SSRM – Basic Performance

Firstly, the p-type calibration sample is measured to investigate the repeatability of SSRM measurements. Figure 1 shows that excellent repeatability is achieved in SSRM measurements on

silicon. Note that the repeatability is better in the highly doped layers. As a reference, for identical scanning parameters, typically a repeatability of 15-20 % is achieved in air highlighting the added value of high vacuum [3].

Secondly, to assess the resolution of SSRM the buried oxide sample is measured. Figure 2 demonstrates that the 0.5 nm oxide layer embedded in silicon can easily be observed in SSRM measurements as an increase in the resistance. The doubling of the resistance on the thin oxide indicates that the electrical contact radius is similar as the oxide thickness, highlighting a sub-nm resolution [2].

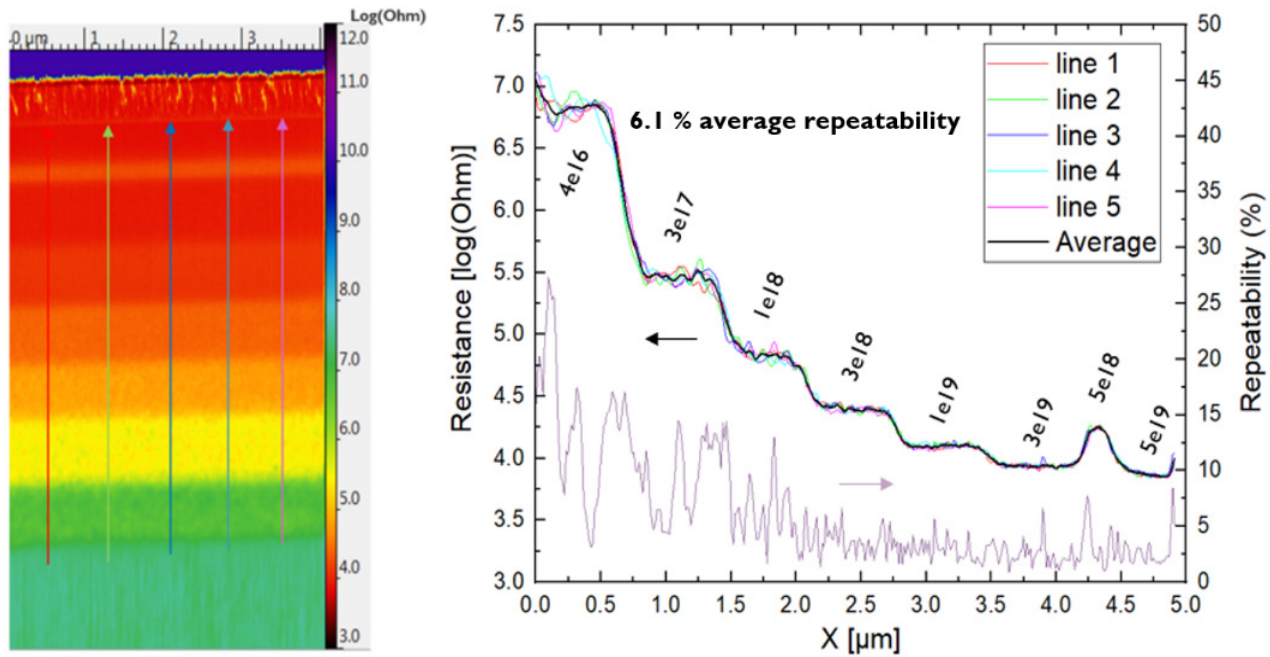


Figure 1: SSRM measurement on a p-type doped silicon calibration sample performed in vacuum. The coloured resistance cross-sections are taken from single line scans and the black line is the average over those 5 scan lines. The repeatability is plotted in purple (right Y-axis).

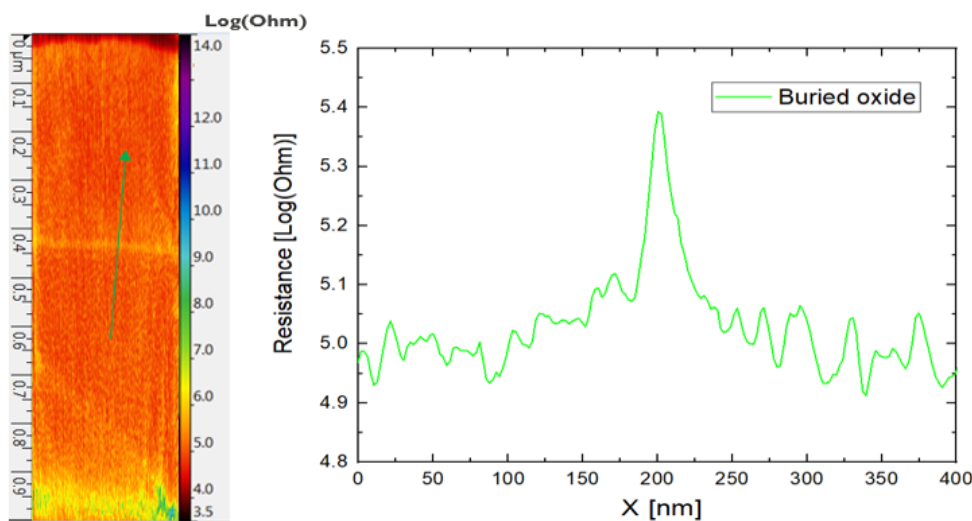


Figure 2: High resolution SSRM measurement on a 0.5 nm oxide layer sandwiched in between highly doped Si and poly Si layers. The resistance cross-section is taken from a single scan line.

Finally, the p-type calibration sample is measured in air and in vacuum with the same probe to verify the advantages of performing SSRM measurements in a vacuum environment. The results are summarized in Figure 3. As expected, in order to obtain an image of similar quality, the applied force to the tip required for a good electrical tip-sample contact had to be increased by almost 50 % when moving from vacuum to ambient environment. This observation suggests that the metallic pocket below the tip apex is induced at

a lower pressure in vacuum as compared to in air. Therefore, measurements in vacuum environment can be performed with a lower force applied to the tip which will result in less tip wear and thus higher resolution [2].

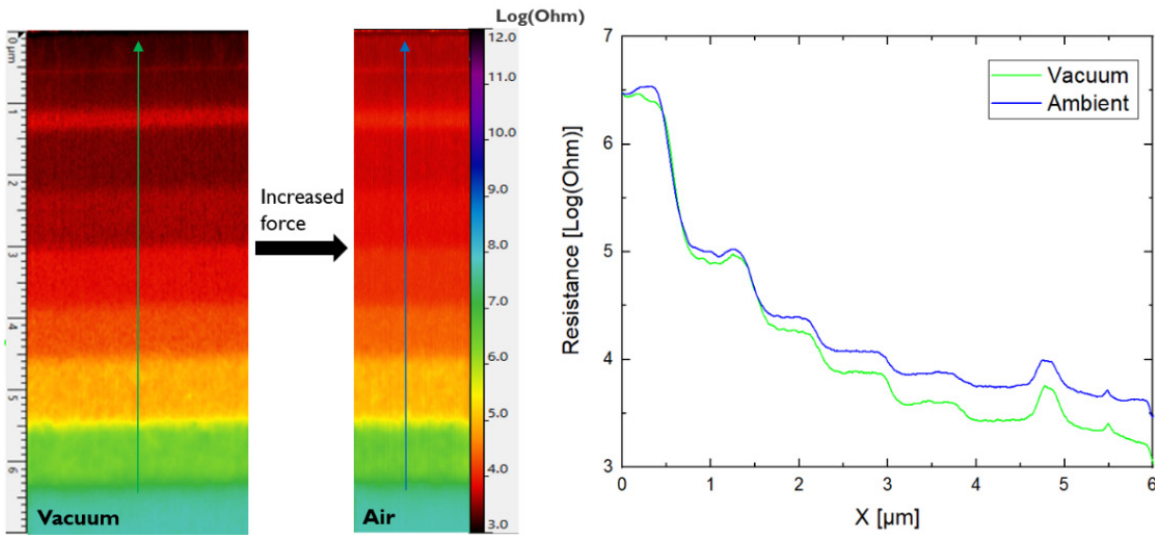


Figure 3: SSRM measurements on a p-type doped silicon calibration sample performed in vacuum and in air with the same probe. The resistance cross-sections are the average over 50 scan lines.

From the results shown above it can be concluded that the repeatability and resolution of SSRM measurements performed on the Park NX-Hivac AFM are state of the art, and that the vacuum conditions in the chamber are beneficial for conducting repeatable SSRM experiments.

The carrier concentration map is calculated from the resistance map by using the calibration curve that is shown in Figure 5. The resistance data points are taken from the average resistance values measured over the 5 layers with known doping levels. The calibration curve is obtained by interpolation of these data points.

## SSRM – Device measurements & calibration

In general, the calibration samples allow to convert the resistance map of an unknown sample to a carrier concentration map. To do so, the calibration sample is measured with the same probe and scan parameters as the measurement on the sample of interest. As an example, in Figure 4, the resistance and carrier concentration maps of an n-type doped silicon layer in a solar cell are shown.

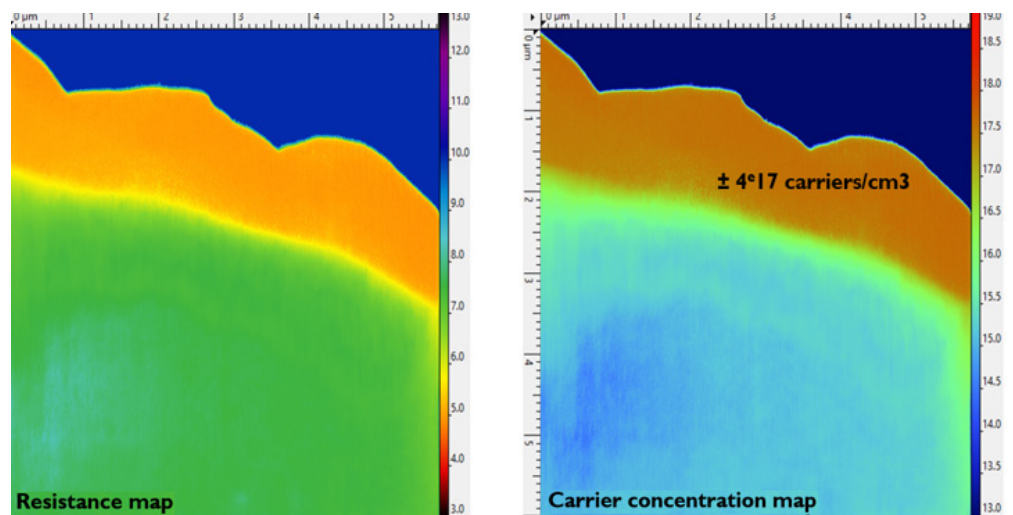


Figure 4: SSRM resistance and carrier concentration maps of an n-type doped silicon layer in a solar cell sample. Is in the calibration sample.

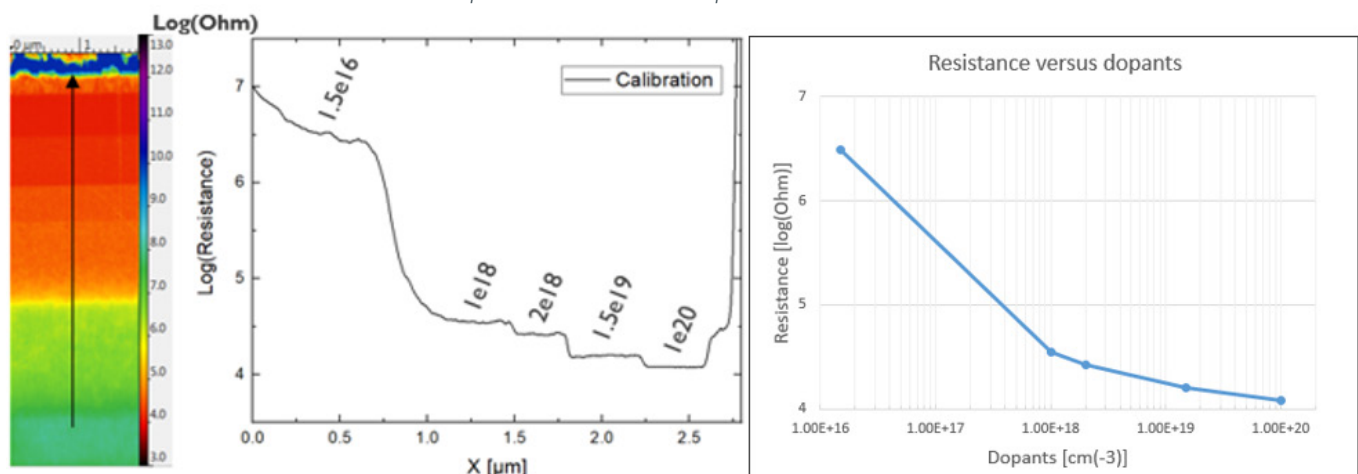


Figure 5: SSRM measurement on an n-type doped silicon calibration sample. The resistance cross-section is taken from the average of 50 scan lines. The resistance versus dopants data points are taken from the average resistance values measured over the 5 layers with known doping levels in the calibration sample.

It can be concluded that the good measurement repeatability on both the sample and the standard allows for an accurate determination of the active carrier concentration in a sample with unknown carrier levels.

## SCM

The n-type doped silicon calibration sample is used to evaluate the performance of SCM on the Park NX-Hivac AFM. This sample has, next to the n-type epitaxial layers, also a p-type doped layer in between the substrate and the n-layers.

Figure 6 shows respectively the dC/dV amplitude and the dC/dV phase map obtained from an SCM measurement on the n-type calibration sample. From the phase map, one can clearly distinguish the n and p-layers. The various n-type layers with different doping concentrations show also a clear contrast in the dC/dV amplitude map. These results demonstrate the carrier concentration sensitivity and the carrier type sensing capability of SCM, even though the spatial resolution is not as good as in SSRM.

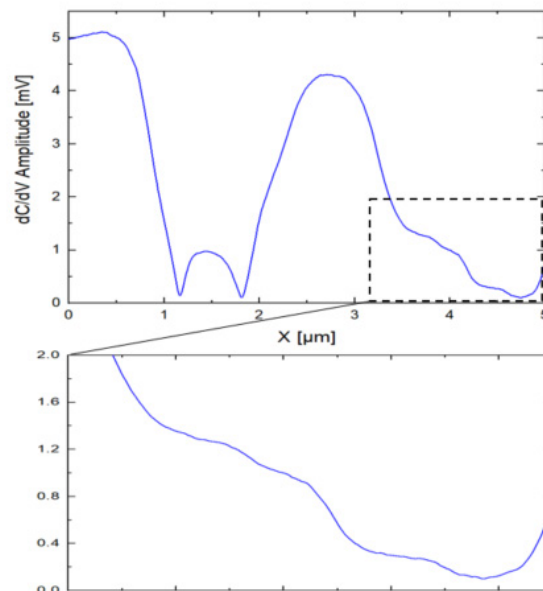
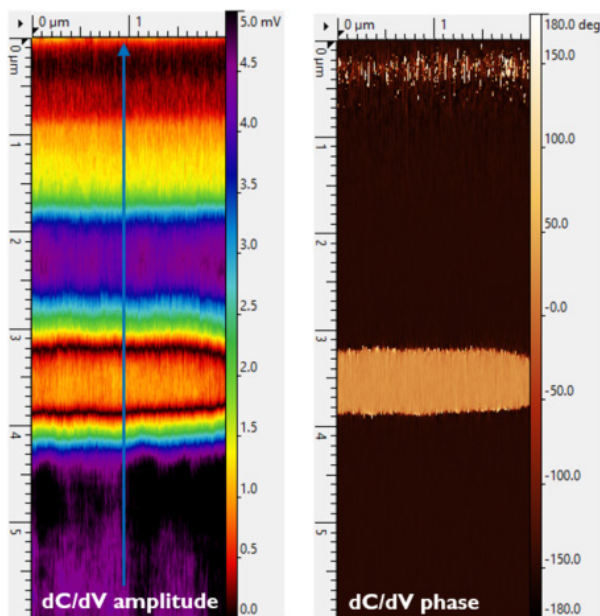


Figure 6: SCM dC/dV amplitude and phase measurements on n-type doped silicon calibration sample. The dC/dV amplitude cross-section is taken from the average of 50 scan lines

Besides Si, another interesting application of SCM is on III-V material stacks. In Figure 7 the results of an SCM measurement on a doped InGaAs stack are shown and they allow to extract information about the carrier concentration and the carrier type.

## Conclusions

This study shows that scanning spreading resistance microscopy (SSRM) and the scanning capacitance microscopy (SCM) can meet the challenges of carrier profiling the state-of-the-art devices entering the sub 10 nm nodes given the right microscopy tool. This investigation found that Park NX-Hivac is the powerful tool that meets the challenges of ever shrinking devices with its implementation of electrical SPM modes, including SSRM and SCM, in a high vacuum environment. Furthermore, we conclude that the use of Park NX-Hivac vacuum aids significantly to reduce the noise, resulting in an average repeatability of 6.1 % for SSRM measurements.

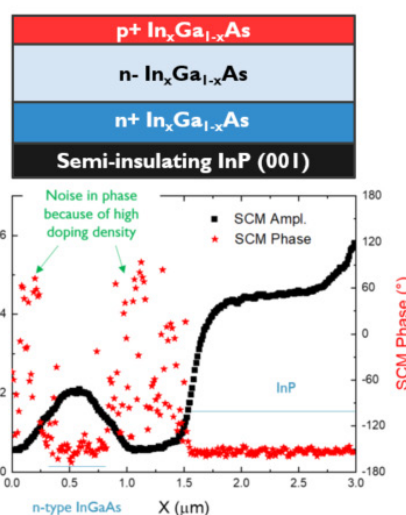
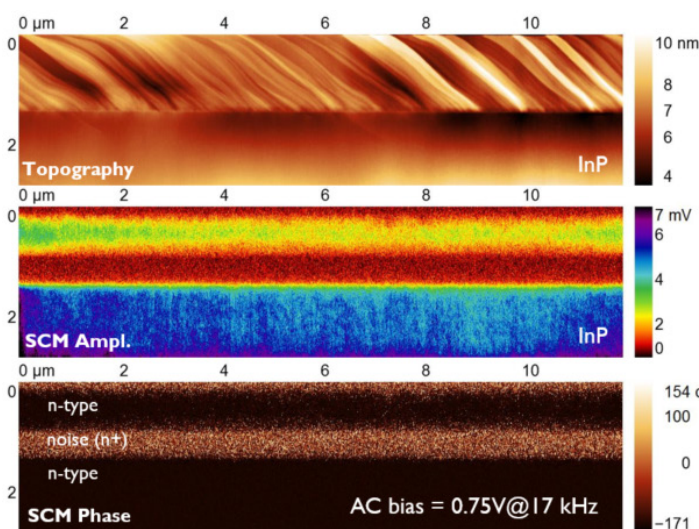


Figure 7: SCM measurement on a doped InGaAs stack. The dC/dV amplitude and phase cross-sections are taken from the average of 100 scan lines.

## References

[1] Park NX-Hivac, Retrieved from <https://parksystems.com/products/small-sample-afm/park-nx-hivac?highlight=WyJueC1oaXZhYyIsIm54LWhpdmFjJ3MiXQ==>

[2] Hantschel, T., et al. Diamond scanning probes with sub-nanometer resolution for advanced nanoelectronics device characterization, *Microelectronic Engineering* 159, 46-50 (2016).

[3] Eyben, P. et al. *Fundamentals of Picoscience, Subnanometer Characterization of Nanoelectronic devices*. Edited by Sattler, K.D., CRC Press (2014)

For more information, please visit: [www.parksystems.com](http://www.parksystems.com)

Park Systems Europe GmbH  
Schildkrötstrasse 15, 68199 Mannheim, Germany  
+49 (0) 621 490896-50  
[pse@parksystems.com](mailto:pse@parksystems.com)

